CHIN. PHYS. LETT. Vol. 35, No. 8 (2018) 083101

Lithium/Silver-Doped Cu_2ZnSnS_4 with Tunable Band Gaps and Phase Structures: a First-Principles Study *

Jun Zhang(张军)[1], Jun Liao(廖峻)[1], Le-Xi Shao(邵乐喜)[1],
Shu-Wen Xue(薛书文)[1**], Zhi-Guo Wang(王治国)[2**]

[1]*School of Physical Science and Technology, Lingnan Normal University, Zhanjiang 524048*
[2]*School of Electronics Science and Engineering, Center for Public Security Technology, University of Electronic Science and Technology of China, Chengdu 610054*

(Received 18 April 2018)

Doping is an effective approach for improving the photovoltaic performance of Cu_2ZnSnS_4 (CZTS). The doping by substitution of Cu atoms in CZTS with Li and Ag atoms is investigated using density functional theory. The results show that the band gaps of $Li_{2x}Cu_{2(1-x)}ZnSnS_4$ and $Ag_{2x}Cu_{2(1-x)}ZnSnS_4$ can be tuned in the ranges of 1.30–3.43 and 1.30–1.63 eV, respectively. The calculation also reveals a phase transition from kesterite to wurtzite-kesterite for $Li_{2x}Cu_{2(1-x)}ZnSnS_4$ as x is larger than 0.9. The tunable band gaps of $Li_{2x}Cu_{2(1-x)}ZnSnS_4$ and $Ag_{2x}Cu_{2(1-x)}ZnSnS_4$ make them beneficial for achieving band-gap-graded solar cells.

PACS: 31.15.A−, 71.55.Gs, 78.20.−e DOI: 10.1088/0256-307X/35/8/083101

Developing cost-effective and highly efficient solar cells is essential to satisfy the rising global demand for sustainable energy. The quaternary semiconductor Cu_2ZnSnS_4 (CZTS) and its derived compounds have attracted a great deal of attention due to their earth-abundant, environmentally benign and non-toxic elements, high absorption coefficients, proper optical band gaps, and high theoretical conversion efficiency (32.2%).[1] CZTS has been considered to be a promising photovoltaic (PV) absorber material for solar cells. Under laboratory conditions, the best recorded efficiencies of $Cu_2ZnSn(S,Se)_4$ (CZTSSe) and CZTS cells are ∼12.6%[2] and ∼9.2%,[3] respectively. For the time being, the efficiency of CZTS based solar cells is still far below the theoretically expected value. The low open-circuit voltage (V_{OC}) of CZTS restricts its commercial applications. The abundant Cu-Zn antisite defects in CZTS are considered to be one of the origins of the low efficiency value obtained by experiments, leading to it being much lower than the theoretical value.[4]

Doping is an effective approach for reducing the Cu-Zn antisite defects and improving the PV performance, such as improving the V_{OC} and the film conductivity of CZTS, and preventing the formation of harmful secondary phases.[5–7] Su *et al.*[8] reported that the power conversion efficiency can be improved significantly from 5.30% to 9.24% with appropriate concentration of Cd substitution for Zn. Device efficiency was enhanced from ∼3% to 6% by Ge substitution for Zn.[9] Na doping could also have the potential to fabricate highly efficient CZTS thin film solar cells,[10] by promoting the growth of larger crystal grains and the conductivity of CZTS.[11] Fully substituting of Zn by other transition metal atoms such as Fe and Mn has also been explored with similar structures. The substitution can help in tuning the optoelectric properties of CZTS, since the substitution may lead to an improvement in the band gap from 1.0 to 1.5 eV and may suppress the formation of the secondary phases.[12] Replacing Cu with equivalent elements with larger radii is also considered to be one effective method to reduce the Cu-Zn antisite defects. Since the covalent radius of Ag (∼0.153 nm) is larger than that of Zn atoms, $Ag_2ZnSnSe_4$ has been predicted to be a promising alternative to CZTSSe for reducing the Cu-Zn antisite defects.[13] It was reported that substitution Ag for Cu in CZTS can lead to a V_{OC} improvement of 50 mV and an absolute efficiency increase of 2.4%.[14] Additionally, it was found experimentally that Li doping can reduce the Cu-Zn disorder in a manner similar to the Ag doping.[15]

Furthermore, the crystal structure and band gap of CZTS can be tuned by changing the substitution elements and their concentrations. For instance, Ge-doped materials have a smaller bandgap than their Ge-free counterparts.[16] The tunable bandgap is beneficial for designing band-gap-graded absorber layers. Since both Ag and Li dopings can reduce the Cu-Zn antisite defects, in this work, we have systematically studied the crystal and electronic structures of CZTS doped by Li and Ag, employing density functional theory (DFT). It is found that the crystal structure and band characteristic can also be tuned by the Li and Ag dopings.

The crystal structures, electronic characteristics, and optical adsorptions were calculated based on the DFT as implemented in the VASP code,[17] in which

*Supported by the National Natural Science Foundation of China under Grant No 61674073, the Science and Technology Planning Project of Guangdong Province under Grant No 2017A050506056, the Key Basic and Applied Research Project of Guangdong Province under Grant No 2016KZDXM021, and the Project of International as well as Hongkong, Macao and Taiwan Science and Technology Cooperation Innovation Platform in Universities in Guangdong Province under Grant No 2015KGJHZ028.
**Corresponding author. Email: xueshuwen@263.net; zgwang@uestc.edu.cn
© 2018 Chinese Physical Society and IOP Publishing Ltd

the plane-wave basis set was used with an energy cutoff of 520 eV. The exchange-correlation energy was described by the generalized gradient approximation using the Perdew–Burke–Ernzerhof (PBE) version. The projector augmented wave method was used to describe the electron-ion interaction.[18] The band gap and optical absorption were calculated with the Heyd–Scuseeria–Ernzerhof hybrid functional[19] with the standard screening parameters of 0.2 (HSE06). The calculations were performed for $Li_{2x}Cu_{2(1-x)}ZnSnS_4$ and $Ag_{2x}Cu_{2(1-x)}ZnSnS_4$ alloys with $x = 0.00$, 0.25, 0.50, 0.75, and 1.00 in the 16-atom supercell. For the Brillouin-zone integration, we used k-point meshes that are equivalent to the $4 \times 4 \times 2$ Monkhorst-Pack scheme[20] for the primitive cell.

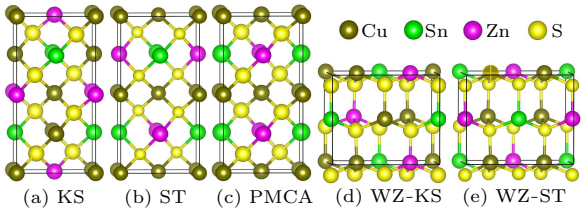

Fig. 1. Crystal structure representations of (a) KS, (b) ST, (c) PMCA, (d) WZ-KS, and (e) WZ-ST.

The quaternary compounds were designed by the cation substitution in ternary system I–III–VI_2, which obeys the octet rule.[21] As a result of increasing elements, quaternary compounds may have more structural configurations. Among these quaternary crystal structures, five fundamental configurations have been reported with the smallest cells and the lowest energies, including the kesterite (KS), stannite (ST), primitive-mixed Cu-Au (PMCA), wurtzite-kesterite (WZ-KS), and wurtzite-stannite (WZ-ST).[22] Figure 1 shows the unit cells of the KS, ST, PMCA, WZ-KS, and WZ-ST structures. For all the structures, S atoms are coordinated with four cations, and each cation is tetrahedrally surrounded by four S ions. There are two inequivalent sites, i.e., the Wyckoff 2a and 2c sites in the KS structure, which are occupied by the Cu atoms, while Zn, Sn, and S atoms occupy 2b, 2d, and 8g sites, respectively. In the ST structure, Cu, Zn, and Sn atoms occupy the Wyckoff 4d, 2a, and 2b sites, respectively, while S atoms occupy the 8i sites. Cu, Zn, Sn, and S atoms are at the Wyckoff 2f, 1d, 1a, and 4n sites in the PMCA structure, respectively. The WZ-derived structures have an $ABABAB$ stacking sequence, while KS and ST structures exhibit an $ABCABC$ stacking sequence. The difference between WZ-derived and KS (ST) structures is a sequential $\pi/3$ rotation of the C and above layers. All simulations were performed in a 16-atom supercell which includes 4 Cu atoms. As 0, 1, 2, 3, and 4 Cu atoms are substituted by Li/Ag atoms, the compounds $Li_{2x}Cu_{2(1-x)}ZnSnS_4$ and $Ag_{2x}Cu_{2(1-x)}ZnSnS_4$ with $x = 0.00$, 0.25, 0.50, 0.75, and 1.00 are formed. All the compounds were analyzed for the five crystalline structures. To describe the site substitution, all symmetrically inequivalent configurations have been considered.

To compare the relative stabilities of these structures, the calculated total energies for each phase for CZTS, LZTS, and AZTS are listed in Table 1. From the total energy, we can find that the KS structure is the most stable for CZTS. The total energies of ST, PMCA, WZ-KS, and WZ-ST phases are respectively 2.77, 3.73, 6.30, and 3.48 meV/atom higher than the KS structure, which are close to the previous reports.[23] For LZTS, the total energy of WZ-KS is 0.54 meV/atom smaller than that of KS, which indicates that WZ-KS is the energetically stable structure for the LZTS. Similar to CZTS, the KS is still the most stable configuration in AZTS, while the WZ-KS structure is 1.59 meV/atom higher than the KS structure in energy. It can be seen from Table 1 that $Ag_{2x}Cu_{2(1-x)}ZnSnS_4$ keeps the KS structure while a phase transition from KS to WZ-KS occurs in $Li_{2x}Cu_{2(1-x)}ZnSnS_4$, when the Cu atoms are substituted.

Table 1. Relative total energies (meV/atom) of Cu_2ZnSnS_4, Li_2ZnSnS_4, and Ag_2ZnSnS_4 to the most energetically stable phase among KS, ST, PMCA, WZ-KS, and WZ-ST.

	KS	ST	PMCA	WZ-KS	WZ-ST
CZTS	0.00	2.77	3.73	6.30	3.48
AZTS	0.00	18.63	19.73	1.59	6.75
LZTS	0.54	10.50	11.88	0.00	1.78

Table 2. Calculated substitution energies (eV) and formation enthalpies (eV per formula unit) for the Li/Ag substitution for Cu in CZTS.

	x	.00	0.25	0.50	0.75	1.00
E_f	Li		−1.73	−1.75	−1.76	−1.77
	Ag		0.39	0.32	0.30	0.27
ΔH_f	Li	−3.71	−4.58	−5.46	−6.34	−7.25
	Ag	−3.71	−3.52	−3.39	−3.25	−3.18

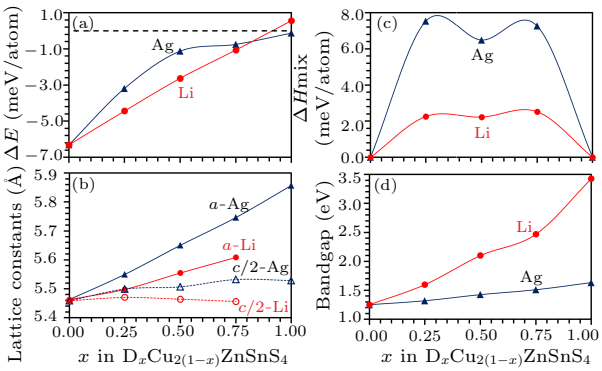

Fig. 2. (a) Total energy difference of $Li_{2x}Cu_{2(1-x)}ZnSnS_4$ and $Ag_{2x}Cu_{2(1-x)}ZnSnS_4$ between KS and WZ-KS with respect to Li and Ag contents. (b) Evolution of lattice parameters (a and $c/2$) of $Li_{2x}Cu_{2(1-x)}ZnSnS_4$ and $Ag_{2x}Cu_{2(1-x)}ZnSnS_4$ with the energetically stable structure. (c) Mixing enthalpies of CZTS and LZTS/AZTS with different Li and Ag contents. (d) Calculated band gaps of $Li_{2x}Cu_{2(1-x)}ZnSnS_4$ and $Ag_{2x}Cu_{2(1-x)}ZnSnS_4$ with the energetically stable structures.

In this work, the doping of equivalent elements (Ag and Li) with Cu atoms is investigated. It is reported

that the Cu-Zn antisite is easy to form in Cu-based compounds, while the Ag-Zn antisite can be suppressed in Ag-based compounds,[24] it is difficult for the Ag to appear at the Zn lattice position. Thus the substitution of Cu by Ag/Li is only considered in this work. The energy differences between KS and WZ-KS structures for the compounds of $Li_{2x}Cu_{2(1-x)}ZnSnS_4$ and $Ag_{2x}Cu_{2(1-x)}ZnSnS_4$, $\Delta E = E_{KS} - E_{WZ-KS}$, are shown in Fig. 2(a). $Ag_{2x}Cu_{2(1-x)}ZnSnS_4$ keeps the KS structure during the whole doping. The WZ-KS structure becomes more stable than KS for $Li_{2x}Cu_{2(1-x)}ZnSnS_4$ as x is larger than 0.9, thus the transition from KS to the WZ-KS structure in $Li_{2x}Cu_{2(1-x)}ZnSnS_4$ occurs at about $x = 0.9$. It should be noticed that the transition from KS to WZ-KS in $Li_{2x}Cu_{2(1-x)}ZnSnS_4$ occurring at about $x = 0.9$ is determined by the 0 K energy difference based on DFT calculations. More advanced *ab initio* techniques[25] or the inclusion of temperature dependent contributions are required to obtain a more accurate value of x. The optimized lattice constants are $a = 5.463$ and $c = 10.918$ Å for CZTS, which are in good agreement with the previous theoretical results.[23] The evolutions of the lattice constants of $Li_{2x}Cu_{2(1-x)}ZnSnS_4$ and $Ag_{2x}Cu_{2(1-x)}ZnSnS_4$ with changing the Li/Ag contents are shown in Fig. 2(b). The lattice parameter a almost increases linearly with the Li/Ag content, whereas the lattice parameter c is slightly increased and decreased by Ag and Li doping, respectively. The dependence of the mixing enthalpy on x has been calculated with $\Delta H_{mix} = E_x - (1-x)E_{CZTS} - xE_{LZTS/AZTS}$, where E_x is the total energy of $Li_{2x}Cu_{2(1-x)}ZnSnS_4$ or $Ag_{2x}Cu_{2(1-x)}ZnSnS_4$, E_{CZTS} is the total energy of CZTS, and $E_{LZTS/AZTS}$ is the total energy of LZTS/AZTS. The mixing enthalpy can be used to describe the energy cost for mixing Li/Ag and Cu atoms in a certain lattice. As shown in Fig. 2(c), both $Li_{2x}Cu_{2(1-x)}ZnSnS_4$ and $Ag_{2x}Cu_{2(1-x)}ZnSnS_4$ have an upward bowing in their ΔH_{mix} dependence on the Li/Ag contents, which indicates that they prefer the phase separation into CZTS and LZTS/AZTS at zero temperature. One can notice that ΔH_{mix} of $Li_{2x}Cu_{2(1-x)}ZnSnS_4$ is lower than that of $Ag_{2x}Cu_{2(1-x)}ZnSnS_4$ over the full range of the Li/Ag content with the typical value of 2.5 meV/atom, which means that Li-doping is much more easily realized than Ag-doping. The substitution energy of Li/Ag substitution for Cu in CZTS is determined using the equation[26] $E_f = (E_{doped} - E_{CZTS} - n\mu_{Li/Ag} + n\mu_{Cu})/n$, where E_{doped} and E_{CZTS} are the total energies of CZTS with and without Li/Ag doping, respectively, $\mu_{Li/Ag}$ and μ_{Cu} are the chemical potentials of the elements Li/Ag and Cu, and n is the number of atoms removed out or added into the system. Since the chemical potential depends on the synthesis condition, in this work, the chemical potential for these elements at their equilibrium elemental solids are considered. The calculated substitution energies are listed in Table 2. The substitution energy is negative for the Li substitution for Cu, indicating that the Li doping is controlled by the availability of Li, which is in agreement with the previous reports of incorporation of Li/Na into CZTS.[27,28] The formation energy of Li doping is correspondingly lower than that of Ag doping, which accords to the results of the mixing enthalpy calculation mentioned above, Li-doping is more easily realized than Ag-doping in CZTS. To verify that doped CZTS can be synthesized in an experiment, the formation enthalpy of doped CZTS is calculated using $\Delta H_f = E_{doped} - x\mu_{Li/Ag} - (2-x)\mu_{Cu} - \mu_{Zn} - \mu_{Sn} - 4\mu_S$, where E_{doped} is the total energy of CZTS with Li/Ag doping, $\mu_{Li/Ag}$, μ_{Cu}, μ_{Sn}, and μ_S are the chemical potentials of the elements Li/Ag, Cu, Sn, and S in their stable bulk states, respectively. The calculated formation enthalpies are listed in Table 2. The formation enthalpies of $Li_{2x}Cu_{2(1-x)}ZnSnS_4$ and $Ag_{2x}Cu_{2(1-x)}ZnSnS_4$ are both negative, which indicate that these alloys can be synthesized experimentally. It can also be seen from Table 2 that the formation enthalpy of $Li_{2x}Cu_{2(1-x)}ZnSnS_4$ is smaller than that of $Ag_{2x}Cu_{2(1-x)}ZnSnS_4$, indicating that Li-doping is easier than Ag-doping in CZTS in an experiment.

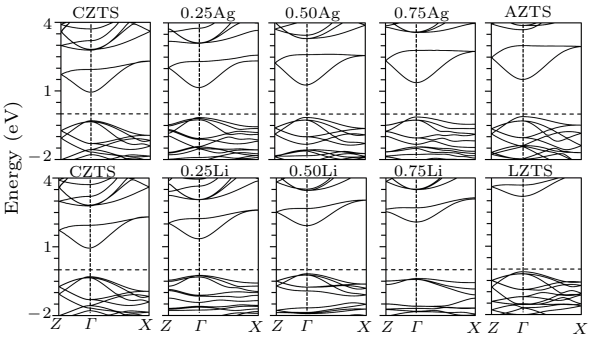

Fig. 3. Band structures of $Li_{2x}Cu_{2(1-x)}ZnSnS_4$ and $Ag_{2x}Cu_{2(1-x)}ZnSnS_4$. The Fermi-level is set to be zero.

The band structures of $Li_{2x}Cu_{2(1-x)}ZnSnS_4$ and $Ag_{2x}Cu_{2(1-x)}ZnSnS_4$ are shown in Fig. 3. All the materials are found to be direct bandgap semiconductors with both valence band maximum (VBM) and conduction band minimum (CBM) located at the Γ point. The bandgap of CZTS is 1.3 eV, which is very close to some previous reports.[29] The evolution of the bandgap upon Li/Ag substitution is shown in Fig. 2(d). It clearly shows that the bandgap increases from 1.3 eV to 3.43 eV and 1.63 eV as Cu is fully substituted by Li and Ag, respectively.

The total and partial density of states (PDOS) of CZTS, AZTS, and LZTS at their stable configurations are shown in Fig. 4. It can be seen from the PDOS of CZTS that the VBM is mainly composed of Cu-3d and S-3p states, and the CBM consists of an unoccupied antibonding orbital of Sn-5s and S-3p. The VBM of AZTS is composed of Ag-4d and S-3p states, while the CBM of AZTS is composed of Sn-5s, S-3p, and Ag-5s states. For the LZTS, the VBM is mainly contributed by Li-3p, Zn-4d, and S-3p, while the CBM

is contributed by Sn-5s, S-3p, Li-3s, and Li-3p states. The bandgap in CZTS is defined by the hybridization of Cu-3d and S-3p states that overwhelmingly dominate the VBM and the hybridization of Sn-5s and S-3p at the CBM. In the Li-doped CZTS, the VBM has a modest contribution from the Li-3p state, and Li-3s and Li-3p states contribute to the CBM, but the S-3p state dominates the whole Fermi level region and overlaps fully with Li-3s and Li-3p states. The energy level of the CBM depends on the distance between Sn and S atoms. The higher the energy level of the CBM is, the wider the bandgap is. The average Sn-S bonding lengths are 2.47, 2.45, and 2.43 Å in CZTS, AZTS, and LZTS, respectively. The decrease of bonding lengths induces stronger hybridization and pushes the CBM level to higher energy, leading to the increase of the bandgap.

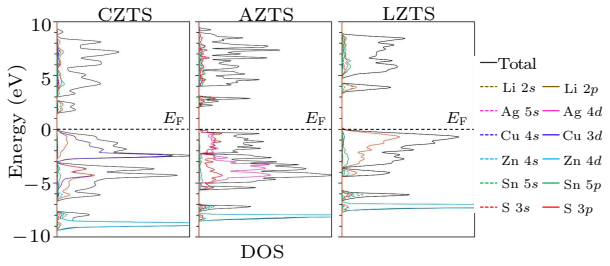

Fig. 4. Total and partial density of states (PDOS) of CZTS, AZTS, and LZTS. The Fermi-level is set to be zero.

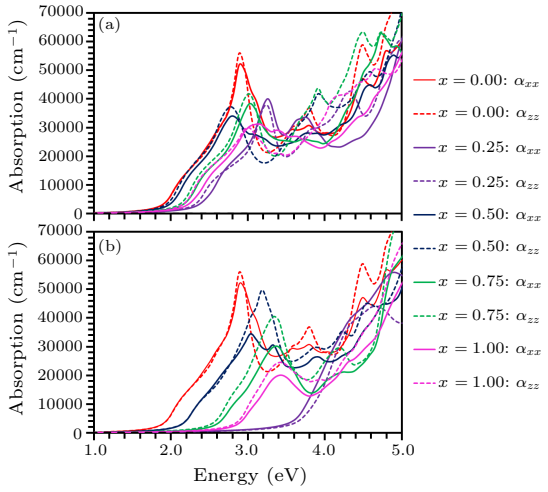

Fig. 5. Calculated absorption coefficient in the visible light region of $Li_{2x}Cu_{2(1-x)}ZnSnS_4$ (a) and $Ag_{2x}Cu_{2(1-x)}ZnSnS_4$ (b).

The optical absorption spectra of $Li_{2x}Cu_{2(1-x)}ZnSnS_4$ and $Ag_{2x}Cu_{2(1-x)}ZnSnS_4$ have been calculated, as shown in Fig. 5, in which the solid and dashed lines represent the adsorption coefficients perpendicular (xx) and parallel (zz) to the c-axis, respectively. The adsorption coefficient perpendicular to the c-axis is smaller than that parallel to the c-axis, which indicates the anisotropy of the absorption coefficient. The calculated spectrum of CZTS is in good agreement with the experimental one.[30] It is clear that the adsorption edge is blue shifted as the Li- and Ag-contents increase, which is consistent with the evolution of the bandgap with Li- and Ag-contents. The adsorption coefficients of the studied materials rise sharply as the photon energy is higher than their bandgaps. In the photon energy range of 2.5–3.5 eV, the adsorption coefficient of the doped-CZTS is slightly lower than that of the corresponding CZTS absorber layer. However, they also have a considerable adsorption coefficient ($2–3\times10^4$/cm). Because the solar spectrum has high intensity in the energy range of 1–3.5 eV, these materials can be used as the absorber layer in solar cells.

Although the optical adsorption of materials is mainly determined by the band structure, it strongly depends on the joint density of states near the VBM and CBM. As the interaction of a photon with electrons can be described in terms of time-dependent perturbations of the electronic ground states, thus the optical absorption in the UV-visible light region is determined by the electronic states near the VBM and CBM. It can be clearly seen from Fig. 5 that the adsorption spectrum of CZTS has one main peak at 2.88 eV with one shoulder at 2.10 eV, which is in the visible light region. The adsorption below 2 eV can be assigned to the transition from Cu-3d/S-3p states to Sn-5s/S-3p states, and the peaks around 3.0 eV can be assigned to the transition from Cu-3d/S-3p states to Sn-5p/Zn-4s/Cu-4s/S-3p states.[31] The adsorption peaks shift to higher energy with increasing the doping concentration, which is induced by the increase of the bandgap, Sn-5s/S-3p states move up in energy. It has been confirmed that one effective approach to improve the efficiency of a CZTS based solar cell is developing the bandgap graded solar cells.[32] The tunable adsorptions of $Li_{2x}Cu_{2(1-x)}ZnSnS_4$ and $Ag_{2x}Cu_{2(1-x)}ZnSnS_4$ make them beneficial for achieving the bandgap-graded solar cells.

In conclusion, first-principles calculations have been carried out to study the crystal structures, electronic characteristics, and optical adsorption properties of CZTS doped by Li and Ag atoms. CZTS can keep the KS structure with and without Ag doping, while a transition from KS to WZ-KS structure occurs in $Li_{2x}Cu_{2(1-x)}ZnSnS_4$ as x is larger than 0.9. The bandgaps of $Li_{2x}Cu_{2(1-x)}ZnSnS_4$ and $Ag_{2x}Cu_{2(1-x)}ZnSnS_4$ can be tuned in the ranges of 1.30–3.43 and 1.30–1.63 eV, respectively. The tunable bandgaps of $Li_{2x}Cu_{2(1-x)}ZnSnS_4$ and $Ag_{2x}Cu_{2(1-x)}ZnSnS_4$ make them beneficial for achieving the bandgap-graded solar cells.

References

[1] Shockley W and Queisser H J 1961 *J. Appl. Phys.* **32** 510
[2] Wang W, Winkler M T, Gunawan O, Gokmen T, Todorov T K, Zhu Y and Mitzi D B 2014 *Adv. Energy Mater.* **4** 1301465
[3] Sun K, Yan C, Liu F, Huang J, Zhou F, Stride J A, Green M and Hao X 2016 *Adv. Energy Mater.* **6** 1600046-n/a
[4] Scragg J J S, Choubrac L, Lafond A, Ericson T and Platzer-Björkman C 2014 *Appl. Phys. Lett.* **104** 041911
[5] Altamura G, Wang M and Choy K L 2016 *Sci. Rep.* **6** 22109

[6] Pianezzi F, Reinhard P, Chirila A, Bissig B, Nishiwaki S, Buecheler S and Tiwari A N 2014 *Phys. Chem. Chem. Phys.* **16** 8843
[7] Han M, Zhang X and Zeng Z 2017 *Phys. Chem. Chem. Phys.* **19** 17799
[8] Su Z, Tan J M R, Li X, Zeng X, Batabyal S K and Wong L H 2015 *Adv. Energy Mater.* **5** 1500682
[9] Khadka D B, Kim S and Kim J 2016 *J. Phys. Chem.* C **120** 4251
[10] Yang Y, Kang X, Huang L, Wei S and Pan D 2015 *J. Phys. Chem.* C **119** 22797
[11] H L A I N G Oo W M, Johnson J L, Bhatia A, Lund E A, Nowell M M and Scarpulla M A 2011 *J. Electron. Mater.* **40** 2214
[12] Ananthoju B, Mohapatra J, Jangid M K, Bahadur D, Medhekar N V and Aslam M 2016 *Sci. Rep.* **6** 35369
[13] Chagarov E, Sardashti K, Kummel A C, Lee Y S, Haight R and Gershon T S 2016 *J. Chem. Phys.* **144** 104704
[14] Guchhait A, Su Z, Tay Y F, Shukla S, Li W, Leow S W, Tan J M R, Lie S, Gunawan O and Wong L H 2016 *ACS Energy Lett.* **1** 1256
[15] Lafond A, Guillot-Deudon C, Vidal J, Paris M, La C and Jobic S 2017 *Inorg. Chem.* **56** 2712
[16] Ford G M, Guo Q, Agrawal R and Hillhouse H W 2011 *Chem. Mater.* **23** 2626
[17] Kresse G and Furthmuller J 1996 *Comput. Mater. Sci.* **6** 15
[18] Kresse G and Joubert D 1999 *Phys. Rev.* B **59** 1758
[19] Heyd J, Scuseria G E and Ernzerhof M 2003 *J. Chem. Phys.* **118** 8207
[20] Pack J D and Monkhorst H J 1977 *Phys. Rev.* B **16** 1748
[21] Chen S, Gong X G, Walsh A and Wei S H 2009 *Phys. Rev.* B **79** 165211
[22] Chen S, Walsh A, Luo Y, Yang J H , Gong X G and Wei S H 2010 *Phys. Rev.* B **82** 195203
[23] Zhong G, Tse K, Zhang Y, Li X, Huang L, Yang C, Zhu J, Zeng Z, Zhang Z and Xiao X 2016 *Thin Solid Films* **603** 224
[24] Yuan Z G, Cheng S Y, Xiang H J, Gong X G, Walsh A, Park J S, Repins I and Wei S H 2015 *Adv. Funct. Mater.* **25** 6733
[25] Peng H and Lany S 2013 *Phys. Rev.* B **87** 174113
[26] Bai Y, Zhang Q, Luo G, Bu Y, Zhu L, Fan L and Wang B 2017 *Phys. Chem. Chem. Phys.* **19** 15394
[27] Xiao W, Wang J N, Zhao X S, Wang J W, Huang G J, Cheng L, Jiang L J and Wang L G 2015 *Sol. Energy* **116** 125
[28] Elaheh G, Hossein M, Janos K and Claudia F 2015 *J. Phys.* D **48** 482001
[29] Kumar M, Zhao H and Persson C 2013 *Thin Solid Films* **535** 318
[30] Wang W, Shen H L, Jin J L, Li J Z and Ma Y 2015 *Chin. Phys.* B **24** 056805
[31] Zhao Z and Zhao X 2015 *J. Semicond.* **36** 083004
[32] Qi Y F, Kou D X, Zhou W H, Zhou Z J, Tian Q W, Meng Y N, Liu X S, Du Z L and Wu S X 2017 *Energy Environ. Sci.* **10** 2401